Biosensors and Bioelectronics 176 (2021) 112933

Contents lists available at ScienceDirect

Biosensors and Bioelectronics

journal homepage: http://www.elsevier.com/locate/bios

Rational design of direct electron transfer type L-lactate dehydrogenase for the development of multiplexed biosensor

Kentaro Hiraka [a], Wakako Tsugawa [a], Ryutaro Asano [a], Murat A. Yokus [b], Kazunori Ikebukuro [a], Michael A. Daniele [b,c], Koji Sode [c,*]

[a] Department of Biotechnology and Life Science, Graduate School of Engineering, Tokyo University of Agriculture and Technology, 2-24-16 Naka-cho, Koganei, Tokyo, 184-8588, Japan
[b] Department of Electrical & Computer Engineering, North Carolina State University, 890 Oval Dr., Raleigh, NC, 27695, USA
[c] Joint Department of Biomedical Engineering, The University of North Carolina at Chapel Hill, North Carolina State University, Chapel Hill, NC, 27599, USA

ARTICLE INFO

Keywords:
L-lactate oxidase
Direct electron transfer
Fusion protein
Site-directed mutagenesis
Multiplexed biosensor
Biomedical engineering

ABSTRACT

The development of wearable multiplexed biosensors has been focused on systems to measure sweat L-lactate and other metabolites, where the employment of the direct electron transfer (DET) principle is expected. In this paper, a fusion enzyme between an engineered L-lactate oxidase derived from *Aerococcus viridans*, AvLOx A96L/N212K mutant, which is minimized its oxidase activity and *b*-type cytochrome protein was constructed to realize multiplexed DET-type lactate and glucose sensors. The sensor with a fusion enzyme showed DET to a gold electrode, with a limited operational range less than 0.5 mM. A mutation was introduced into the fusion enzyme to increase K_m value and eliminate its substrate inhibition to construct "b2LOxS". Together with the employment of an outer membrane, the detection range of the sensor with b2LOxS was expanded up to 10 mM. A simultaneous lactate and glucose monitoring system was constructed using a flexible thin-film multiplexed electrodes with b2LOxS and a DET-type glucose dehydrogenase, and evaluated their performance in the artificial sweat. The sensors achieved simultaneous detection of lactate and glucose without cross-talking error, with the detected linear ranges of 0.5–20 mM for lactate and 0.1–5 mM for glucose, sensitivities of 4.1 nA/mM·mm^2 for lactate and 56 nA/mM·mm^2 for glucose, and limit of detections of 0.41 mM for lactate and 0.057 mM for glucose. The impact of the presence of electrochemical interferants (ascorbic acid, acetaminophen and uric acid), was revealed to be negligible. This is the first report of the DET-type enzyme based lactate and glucose dual sensing systems.

1. Introduction

L-lactate is a key metabolite in human energy producing processes of glycolysis and oxidative phosphorylation (Bakker et al., 2013). Thus, the anomalous increase of blood L-lactate level causes a lactic acidosis in tissue hypoxia or underlying diseases (Mizock and Falk, 1992). The blood L-lactate level also corresponds to the physiological performance or endurance marker of athletes (Faude et al., 2009). Because of the high correlation between sweat and blood L-lactate level (Karpova et al., 2020), wearable lactate monitoring systems have been paid great attention in recent years (Jia et al., 2013; Gao et al., 2016; Anastasova et al., 2017; Sempionatto et al., 2017; Currano et al., 2018; Yokus et al., 2020).

Enzyme based lactate sensors have been vigorously studied. These include the first generation principle sensors, using oxidases as a molecular recognition elements and measuring oxygen consumption or liberated hydrogen peroxide (Karube et al., 1980; Matsunaga et al., 1982; Clark et al., 1984), and the second generation principle sensors, using artificial electron mediators (Palleschi and Turner, 1990). The second generation based lactate sensor is widely utilized as the disposable type sensors, employing lactate oxidase (LOx) due to its high specificity and stability. LOx is a member of flavin mononucleotide (FMN)-dependent α-hydroxy acid oxidoreductase family (EC: 1.1.3.15). LOx oxidizes L-lactate to pyruvate coupled with FMN reduction in a reductive half-reaction. In the oxidative half-reaction, LOx uses molecular oxygen as a natural electron acceptor to reoxidize FMN. The main concern is an oxygen interference effect with the oxidases (Palleschi and Turner, 1990; Kenausis et al., 1996; Hiraka et al., 2018). The oxygen

* Corresponding author.
E-mail address: ksode@email.unc.edu (K. Sode).

https://doi.org/10.1016/j.bios.2020.112933
Received 31 October 2020; Received in revised form 17 December 2020; Accepted 22 December 2020
Available online 25 December 2020

interference effect is caused by the electron acceptor competition with oxygen and electron mediator in the oxidative half-reaction. The authors have been engaged in the construction of engineered oxidases by introducing mutations to minimize oxidase activities using oxygen as an electron acceptor, whereas keeping or even improving dye-mediated dehydrogenase activities (Kim et al., 2010, 2012; Horaguchi et al., 2012, 2014; Kojima et al., 2013; Hiraka et al., 2020b), including the development of virtually lactate dehydrogenases (LDH) from LOx (Hiraka et al., 2018, 2020a; Lin et al., 2018). Another amperometric enzyme sensor principle is so called third generation biosensors, utilizing the specific dehydrogenases which is capable of a direct electron transfer (DET) from enzyme to electrode (Ferri et al., 2011; Yamashita et al., 2018). This system does not need oxygen or any artificial electron mediators, therefore, it seems to the ideal system. There have been several approaches to develop continuous lactate monitoring system by employing LOx, based on first or second generation principles (Jia et al., 2013; Abrar et al., 2016; Gao et al., 2016; Hickey et al., 2016; Imani et al., 2016; Luo et al., 2018; Ashley et al., 2019; He et al., 2019; Lei et al., 2019; Payne et al., 2019; Terse-Thakoor et al., 2020; Yokus et al., 2020; Wang et al., 2021), focusing to realize wearable sweat lactate sensors. Enzyme sensors employing third generation principle is especially ideal for continuous monitoring, considering that the third-generation principle is operated under low (less than 200 mV vs. Ag/AgCl) oxidation potential which is benefit to minimize the impact of the electrochemically active ingredients, utilizes no electron mediator or oxygen, the use of toxic artificial electron mediators is not necessary, and errors due to variations in the concentration of oxygen in blood samples are eliminated (Lee et al., 2018). However, the number of lactate oxidizing enzymes capable of DET are limited (Treu and Minteer, 2008; Smutok et al., 2017). To solve this problem, our group have proposed 2.5th generation sensing system which uses the mediator modified engineered LOx. The LOx mutant derived from *Aerococcus viridans* (AvLOx Ala96Leu) was rationally designed by introducing Asn212Lys mutation (AvLOx A96L/N212K), to be modified by an electron mediator, 1-[3-(Succinimidyloxycarbonyl)propoxy]-5-ethylphenazinium trifluoromethanesulfonate, or amine reactive phenazine ethosulfate (arPES), thereby achieved the quasi-DET via modified mediator with minimized reactivity for oxygen (Hiraka et al., 2020a). Recently, we have reported the fusion enzymes composed of non-DET-type fungi derived flavin adenine dinucleotide (FAD) dependent glucose dehydrogenases (FADGDH) with heme *b* containing proteins, (Ito et al., 2019a; Yanase et al., 2020). FADGDH does not utilize oxygen as an electron acceptor, therefore, fusion enzyme can transfer electron from FAD to heme *b*, without the competition with oxygen. Considering our current achievement in the construction of virtually lactate dehydrogenases (LDH) from LOx (Hiraka et al., 2018, 2020a; Lin et al., 2018), the creation of fusion enzyme between an engineered LOx which is minimized its oxidase activity and heme harboring protein would be a challenging strategy to develop a DET-type lactate sensing enzyme based continuous lactate monitoring system.

On the other hand, the use of LOx for lactate sensors, suffers from its inherent low K_m value (about 1 mM) together with substrate and product inhibition (Maeda-Yorita et al., 1995; Taurino et al., 2013; Hiraka et al., 2018). Considering the sweat lactate concentration in endurance exercise (up to 43.7 mM) and exhaustive exercise (up to 115.8 mM) (Mitsubayashi et al., 1994), this phenomenon severely affects the sensor signal. This problem limits the detection range of the continuous lactate monitoring system using LOx. Therefore, the creation of an engineered LOx/LDH with altered K_m value and not showing substrate inhibition is needed.

In this paper, we attempted to create DET-type lactate sensing enzyme with expanded dynamic range, and to realize multiplexed DET-type lactate and glucose sensors with the combination of DET-type FADGDH (Sode et al., 1996; Inose et al., 2003; Tsuya et al., 2006; Yamazaki et al., 2008; Yamashita et al., 2013; Lee et al., 2018, 2019; Yoshida et al., 2019) (Scheme 1). DET-type engineered LOx, "b2LOx"

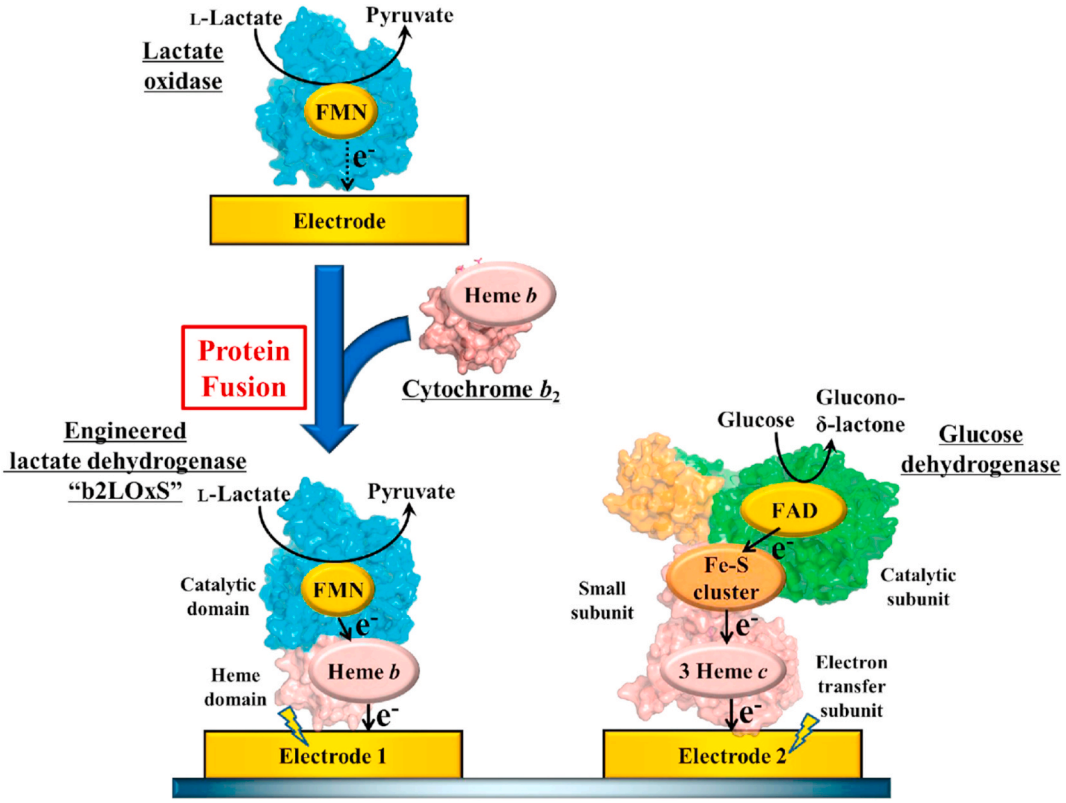

Scheme 1. Schematic illustration of DET-type LOx design and the electrode for simultaneous monitoring of lactate and glucose together with DET-type FAD glucose dehydrogenase.

was developed by fusing flavocytochrome b_2 (Fcb2) heme domain to AvLOx A96L/N212K mutant which was minimized oxidase activity keeping dye-mediated dehydrogenase activity. To avoid substrate inhibition and expand the dynamic range of measurement, we introduced a new mutation, Ala95Ser in AvLOx A96L/N212K mutant, thereby created new fusion enzyme DET-type LDH, designated as "b2LOxS", without substrate inhibition together with increased K_m value. Finally, b2LOxS and DET-type FADGDH was immobilized on multiplexed flexible thin-film gold (Au) electrodes with an outer membrane to limit the diffusion of substrate. Subsequently, the simultaneous measurement of glucose and lactate was achieved in the artificial sweat, based on DET principle, without a cross-talking of the signals, and without significant impact of electrochemical ingredient, thanks to the low oxidation potential for DET-type sensor operation.

2. Materials and methods

2.1. Chemicals and materials

Sodium L-lactate, Polyethylenimine branched (PEI) Mn ~10,000, and poly(ethylene glycol) diglycidyl ether (PEGDGE) Mn 500 were purchased from Sigma-Aldrich (MO, USA). 4-aminoantipyrine (4-AA) and phenazine methosulfate (PMS), D-glucose were obtained from Kanto Kagaku (Tokyo, Japan). *N*-Ethyl-*N*-(2-hydroxy-3-sulfopropyl)-3-methylaniline sodium salt (TOOS) were purchased from Dojindo Laboratories (Kumamoto, Japan). LB broth, 2,6-dichloroindophenol (DCIP) were obtained from Merck (Darmstadt, Germany). Peroxidase were purchased from Amano Enzyme (Gifu, Japan). The Au disk electrodes (ϕ 3 mm), Ag/AgCl reference electrode RE-1B, water-jacketed glass cell, 1 μm polishing diamond, and 0.05 μm polishing alumina were obtained from BAS Inc. (Tokyo, Japan). Multiwalled carbon nanotube (MWCNT) ink (2 wt%) was purchased from Meijo Nano Carbon Co., Ltd. (Aichi, Japan). Cellulose acetate -CA-398-10NF/EP was obtained from Eastman (Tennessee, USA). Platinum wire was purchased from Tanaka Kikinzoku Kogyo K.K. (Tokyo, Japan). FADGDH derived from *Burkholderia cepacia* (BcGDH) was prepared according to the previous studies (Tsuya et al., 2006). All chemicals were reagent grade.

2.2. Design of engineered LOx and recombinant production

For design of the engineered LOx (b2LOx), the structural gene of AvLOx A96L/N212K mutant (Hiraka et al., 2020a) was fused with the structural gene of Fcb2 heme domain derived from *Pichia pastoris* (PpFcb2) by the overlap PCR method with KOD-Plus-Neo DNA polymerase (Toyobo CO., LTD. Osaka, Japan) and primers which were purchased from the Eurofins Genomics Inc. (Tokyo, Japan, Supplementary data, Table SI). PpFcb2 structural gene was PCR amplified from genomic DNA of *Pichia pastoris* KM71 strain (NCBI Reference Sequence: XP_002493685.1). The amplified DNA was inserted into pET30c(+) (Merck KGaA, Darmstadt, Germany) by NdeI and NcoI double restriction enzymes digestion and DNA ligation kit ver.2.1 (Takara Bio Inc. Shiga, Japan). Site-directed mutagenesis was conducted by Quikchange method with KOD-Plus-Neo DNA polymerase and primers which were also purchased from the Eurofins Genomics Inc. (Tokyo, Japan, Supplementary data, Table SI). The template DNA was digested by *Dpn*I (Roche Diagnostics GmbH, Mannheim, Germany) at 37 °C for 2 h. After amplification of these constructed expression vectors by *Escherichia coli* DH5α strain, the inserted structural gene sequences were confirmed by the Eurofins Genomics DNA sequencing service (Tokyo, Japan). *Escherichia coli* BL21 (DE3) were transformed with these constructed expression vectors for AvLOx A96L/N212K mutant, b2LOx, and other mutants. Enzyme recombinant production, purification and mutant screening were performed according to our previous papers (Hiraka et al., 2020a) but a cultivation condition was modified from aerobic to micro-aerobic for cytochrome *b* maturation.

2.3. Enzyme activity assays and spectrum analysis

Enzyme activities were measured according to our previous report (Hiraka et al., 2018, 2020a). Protein concentrations were determined by Bradford assay (Bio-Rad Laboratories, CA, USA).

To evaluate the intra-electron transfer from FMN to heme, spectrum analysis was conducted by V-630 UV-VIS spectrophotometer (JASCO CO., Ltd., Tokyo, Japan) with or without L-lactate. Twenty five U/mL (dehydrogenase activity for 20 mM L-lactate) enzyme solution was prepared with 20 mM potassium phosphate buffer (P.P.B.) pH 7.0 and measured absorption spectrum between 250 and 700 nm with scan rate 1000 nm/min. Then, 20 mM L-lactate was added to the enzyme solution, and the absorption spectrum change of the mixture was monitored at 5, 60, 120, 180, 240, 300, 360, 420, 480, 540 s after addition of L-lactate.

2.4. Fabrication and characterization of enzyme electrodes

Au disk electrodes were polished according to our previous paper (Ito et al., 2019b). After polishing Au disk electrodes, 2 w/w% of MWCNT dispersion 2 μL (40 μg) was dropped onto an inner area of the Au disk electrode (Outer diameter: 6 mm, Inner diameter: 3 mm). After drying for 15 min, 2 units of enzyme solution (dehydrogenase activity for 20 mM L-lactate) was dropped onto the MWCNT layer. After drying for 15 min, 2 μL of the mixed solution with 10 mg/mL PEI and 20 mg/mL PEGDGE was applied onto an enzyme layer and dried for 30 min. To increase the substrate diffusion layer, whole surfaces of electrodes were coated with 6 μL of 3 w/v% cellulose acetate solution containing 1 v/v% water dissolved into the Ethyl formate and cyclohexanone at a ratio of 3:1, and electrodes were dried at least 1 h. The fabricated electrodes were equilibrated in the 20 mM P.P.B. (pH7.0) for 15 min before measurement. Cyclic voltammetry and chronoamperometry was performed using the fabricated enzyme electrodes, Ag/AgCl reference electrode, Pt wire counter electrode, and Uniscan Electrochemical Measurement System. Chronoamperometry was performed using 10 mL of 20 mM P.P.B. (pH 7.0) with successive addition of sodium L-lactate and applied 150 mV vs. Ag/AgCl with continuous stirring.

2.5. Preparation of DET-type multiplexed enzyme sensor with thin-film Au electrodes and simultaneous measurement of lactate and glucose in the artificial sweat

The flexible thin-film Au electrodes were fabricated according to the previous report (Yokus et al., 2020). Among the four working electrodes, two larger electrodes were used for simultaneous lactate and glucose monitoring, as are shown in Fig. 5A; WE4; electrode radius with 1.225 mm for lactate monitoring and WE3; electrode radius with 0.975 mm for glucose monitoring, respectively. Reference electrode was Ag/AgCl ink and counter electrode was Au. First, 2% of MWCNT dispersion was dropped onto the Au working electrode (5.66 μg/mm^2). After drying for 15 min, the b2LOxS and BcGDH were dropped onto the MWCNT layer (3.75 μg/mm^2). After drying for 15 min, the mixed solution with 10 mg/mL PEI and 20 mg/mL PEGDGE was applied onto an enzyme layer (2.83 and 5.66 μg/mm^2) and dried for 30 min. Electrodes were coated three times with 0.5 μL or 0.32 μL of 3 w/v% cellulose acetate solution containing 1 v/v% water dissolved into the cyclohexanone. After drying for at least 1 h, the fabricated electrodes were equilibrated in the 20 mM P.P.B. (pH 7.0) for 15 min before measurement. Chronoamperometry was performed using CE to Ground mode of VSP Electrochemical Measurement System (Bio-Logic Science Instruments Ltd., Seyssinet-Pariset, France) and 10 mL of artificial sweat (pH 5.4) with successive addition of sodium L-lactate or D-glucose (150 mV vs. Ag/AgCl with continuous stirring). Artificial sweat was prepared using the EN1811:2012 standard but it was slightly modified for the L-lactate sensor evaluation (0.5% NaCl, 0.1% KCl, 0.1% Urea, and 2.0 mM D-lactate. The pH value was adjusted to 5.4 using 1 mM ammonium hydroxide) (Kondoh et al., 1992; Liu et al., 2015). The impact of electroactive sweat interferents was

investigated using 10 μM ascorbic acid, 132 μM acetaminophen, and 59 μM uric acid (Harvey et al., 2010; Lee et al., 2017) in the presence of 5 mM L-lactate and 1 mM D-glucose using the artificial sweat. To evaluate the sensor stability, continuous operation was performed by chronoamperometric measurement against 5 mM L-lactate and 1 mM D-glucose for 12 h in the artificial sweat (150 mV vs. Ag/AgCl with continuous stirring). The out-putted amperogram was analyzed by Band reject filter with Welch window. The rejected band frequencies were from 20 mHz to 50 mHz to remove the noise coming from the continuous stirring. This smoothing analyzation was processed by EC-Lab software (Bio-Logic Science Instruments Ltd., Seyssinet-Pariset, France).

3. Results

3.1. Design of the direct electron transfer type enzyme "b2LOx"

As a design of the DET-type enzyme, an oxygen insensitive AvLOx mutant, AvLOx A96L/N212K, was used as a "catalytic domain" and was fused with PpFcb2 heme domain to construct a fusion enzyme designated as b2LOx. The *b*-type heme binding domain and FMN binding catalytic domain are connected with a hinge peptide. This hinge region can move flexible and confer the mobility to these domains. The b2LOx was produced by *E. coli* as a soluble protein, with expected molecular weight (57 kDa) (Supplemental Materials Fig. S1). The newly constructed b2LOx maintained nearly half of the dehydrogenase activity of AvLOx A96L/N212K mutant at each lactate concentration. Both AvLOx A96L/N212K mutant and b2LOx decreased specific activity for more than 20 mM lactate due to substrate inhibition (Supplemental Materials Fig. S2).

To investigate the intra-electron transfer from FMN to heme, the spectrum analysis was conducted with b2LOx before and after addition of lactate. Fig. 1B clearly indicates that, b2LOx showed a peak spectrum at 413 nm, which is corresponding to the Soret band of oxidized heme *b*, which was not found in the spectrum of AvLOx A96L/N212K (Fig. 1A). After the addition of 20 mM lactate, Soret band peak was shifted to 423 nm and spectra peaks at 527 nm and 556 nm were drastically increased (Fig. 1B), which are corresponded to α and β band spectra of reduced heme *b* of Fcb2 (Brunt et al., 1992). These results indicated that b2LOx bound *b*-type heme and showed the intra-electron transfer from FMN to heme after FMN reduction by the lactate oxidation reaction.

3.2. Electrochemical evaluation of b2LOx

The direct electron transfer ability of b2LOx was then evaluated by chronoamperometry, using Au-disk electrodes with b2LOx immobilized in a PEI-PEGDGE crosslinked hydrogel. As shown in the results of chronoamperometry (Fig. 2A and B), the b2LOx immobilized electrodes exhibited lactate concentration dependent current increase up to 2 mM lactate without external electron acceptors, revealing that the fusion enzyme showed DET ability. Although AvLOx A96L/N212K mutant immobilized electrode exhibited a slight DET-type response, its lactate concentration dependency was limited under 0.5 mM lactate, indicating there was significant electron transfer limitation between enzyme and electrode. These results indicated that the fused heme domain drastically enhanced the DET ability of AvLOx A96L/N212K mutant.

3.3. Improvement of linear range of DET-type lactate sensor by introducing mutation on b2LOx and by the employment of an outer membrane

Considering that the electrode with b2LOx showed current increase saturation at lactate concentration higher than 2 mM (Fig. 2B) and limited the linear range by 1 mM, the current performance of DET enzyme was not suitable for the measurement of lactate in biological samples. To overcome this problem, site directed mutagenesis to increase K_m value and also to relieve the substrate inhibition was attempted together with the employment of an outer membrane to limit the substrate diffusion thereby increase the linear range of measurement.

First, a residue, Ala95 in AvLOx was focused, because this residue was reported as crucial for substrate release (Yorita et al., 1996) (Fig. 3A). The Ala95 was substituted to little bulky amino acid residues (Cys, Ser, Val, Thr, Pro) in AvLOx A96L/N212K mutant. Among these mutants, only AvLOx A95S/A96L/N212K mutant kept dye-mediated lactate dehydrogenase activity, whereas other amino acid substitutions resulted drastic decrease in enzyme activity. More remarkably, A95S substitution suggested the possible waive from the substrate inhibition showing increase enzyme activities up to 100 mM; whereas, AvLOx A96L/N212K decreased enzyme activities at lactate concentration higher than 20 mM (Supplemental Materials Figs. S3 and S4 and Table S2). Therefore, this mutation was also introduced into b2LOx and purified for further evaluation. Hereafter, b2LOx with A95S mutation is described as "b2LOxS".

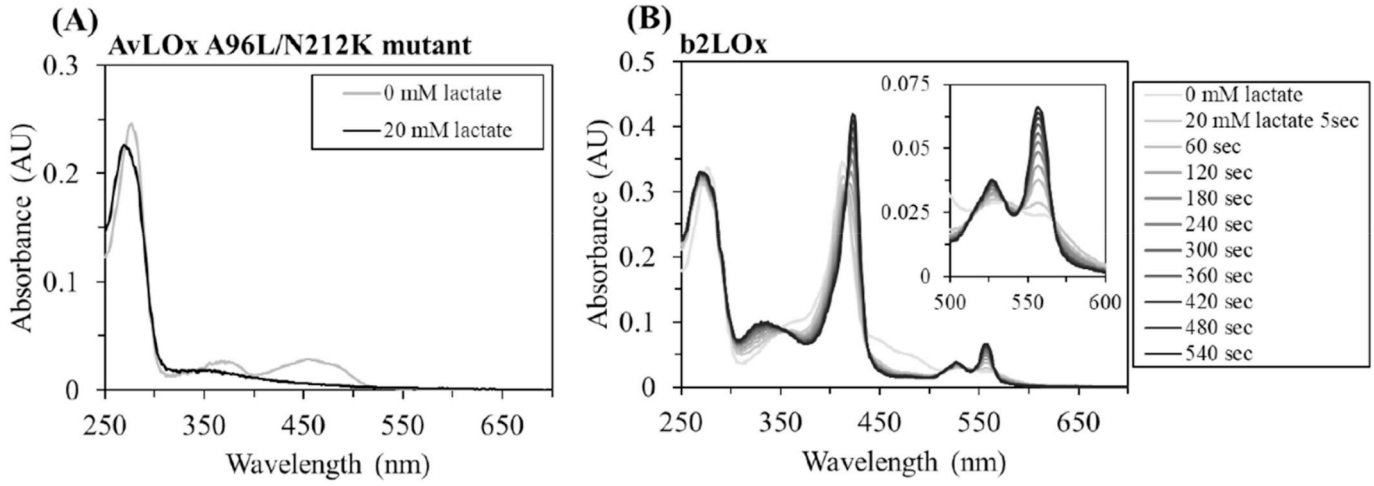

Fig. 1. Spectrum analysis of AvLOx A96L/N212K mutant and b2LOx. The absorbance spectrum of 25 U/ml (A) AvLOx A96L/N212K mutant and (B) b2LOx which is a fusion enzyme between AvLOx A96L/N212K mutant and PpFcb2 heme domain. Most light gray line shows the absorbance spectrums before addition of L-lactate. AvLOx A96L/N212K mutant showed an immediate spectral change after the addition of 20 mM L-lactate (black line). The b2LOx showed time-dependent spectral change after the addition of 20 mM L-lactate (line plot in grayscale). Inset figure shows the absorbance spectrum of b2LOx between 500 and 600 nm to enlarge the spectrum peak at 527 and 556 nm.

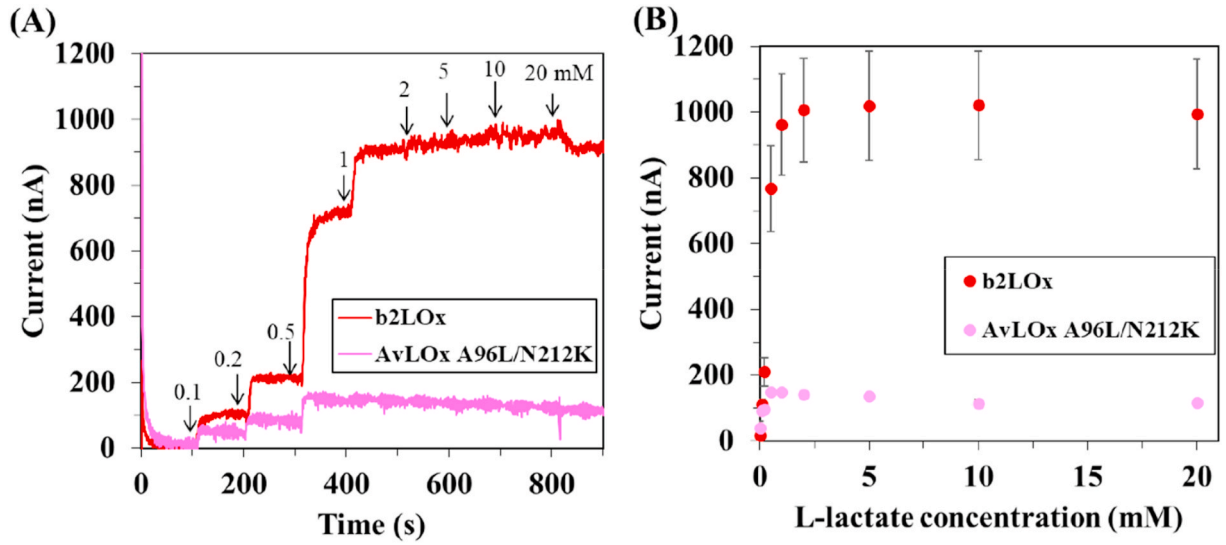

Fig. 2. L-lactate measurement based on chronoamperometry. Chronoamperometry was conducted using the 10 mL of 20 mM PPB pH 7.0 at 37 °C with continuous stirring. Applied potential was 150 mV vs. Ag/AgCl. Chronoamperograms using AvLOx A96L/N212K mutant (pink) or b2LOx (red) immobilized electrode without an outer membrane were shown in (A) and calibration curves were calculated as (B). These experiments were performed by using three different electrodes and error bars showed standard deviation.

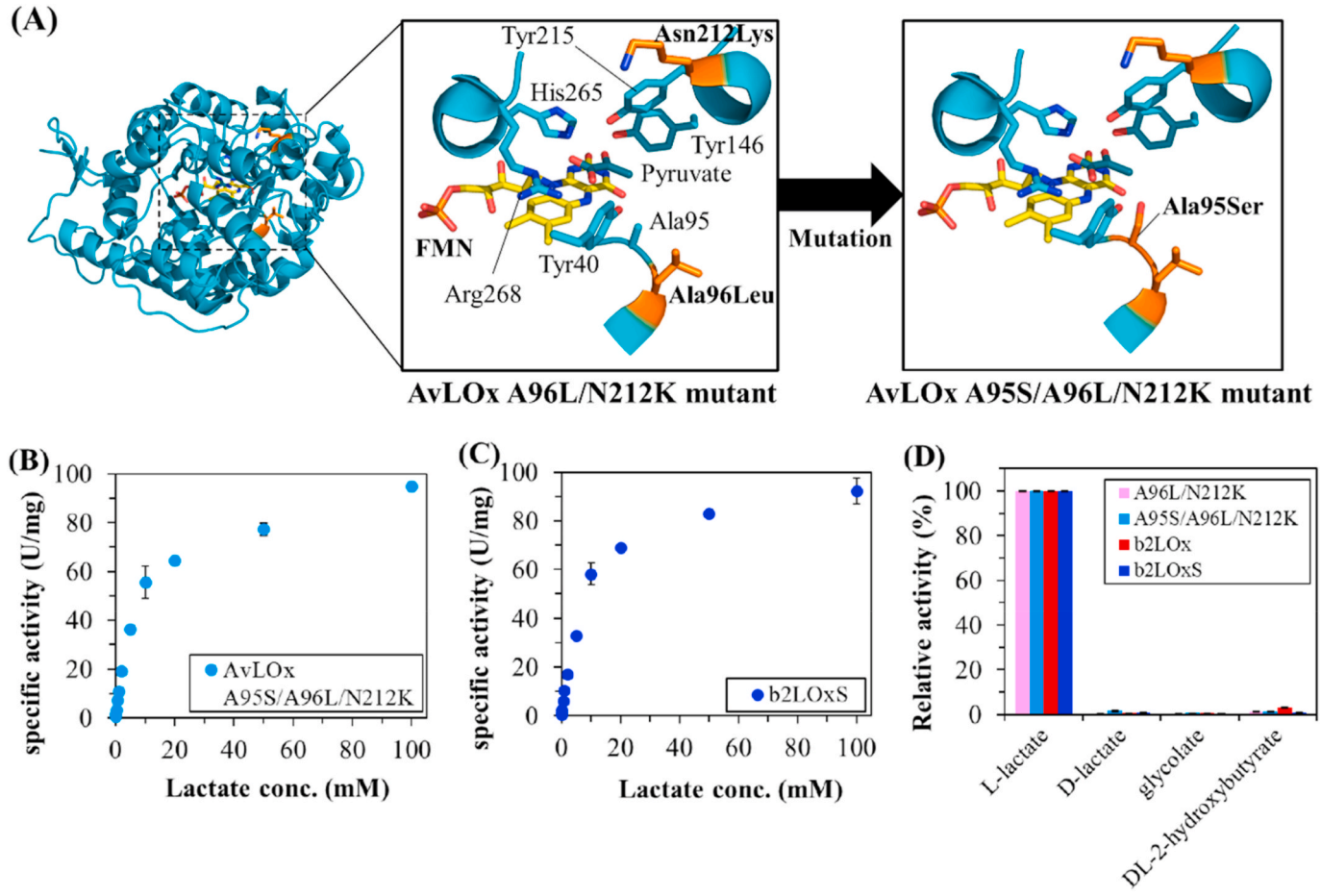

Fig. 3. Dehydrogenase activities of purified AvLOx A96L/N212K mutant and AvLOx A95S/A96L/N212K mutant. (A) Illustration of AvLOx substrate recognition site. The mutants images were prepared using PDB code: 2E77 chain D, PyMOL molecular Graphics System, Version 2.0 Schrodinger, LLC, and its mutagenesis wizard. The dehydrogenase activities toward various L-lactate concentration of (B) AvLOx A95S/A96L/N212K mutant and (C) b2LOxS which is a fusion enzyme between AvLOx A95S/A96L/N212K mutant and PpFcb2 heme domain. (D) Substrate specificities of AvLOx A96L/N212K mutant, AvLOx A95S/A96L/N212K mutant, b2LOx, and b2LOxS toward 20 mM L-lactate, D-lactate, glycolate, and DL-2-hydroxybutyrate. Each experiment was conducted triplicate and error bar showed standard deviation.

The AvLOx A95S/A96L/N212K mutant and b2LOxS were purified and were evaluated their dehydrogenase activities (oxidase activities were not detected) shown in Fig. 3B and C. Comparing with the dehydrogenase activities of AvLOx A96L/N212K mutant and b2LOx (Supplemental Materials Figs. S2A and B), AvLOx A95S/A96L/N212K mutant and b2LOxS showed increasing of the specific activity until 100 mM lactate. Kinetic parameters were summarized in Table 1.

The K_m and V_{max} values of AvLOx A95S/A96L/N212K mutant and b2LOxS were calculated using the specific activity for 0–100 mM lactate. By A95S mutation, AvLOx A96L/N212K mutant increased K_m value from 1.1 mM to 7.9 mM, more than 7-folds increase. Similarly, K_m value of b2LOx increased by A95S mutation from 0.56 mM to 8.6 mM, more than 15-folds increase. More remarkably, K_i value, which represents substrate inhibition of enzyme, was no longer available since no substrate inhibition was observed in both AvLOx A95S/A96L/N212K and b2LOxS. Substrate specificity was also checked using 20 mM D-lactate, glycolate, and DL-2-hydroxybuthylate, however, heme domain fusion or A95S substitution did not affect the substrate specificity (Fig. 3D). These results revealed that A95S mutation relieved substrate inhibition with increased K_m value without loss of the specificity for L-lactate. Therefore, b2LOxS showed the potential for detection of broad lactate concentration based on DET principle. Then, b2LOxS immobilized electrodes were prepared and their performance was evaluated by chronoamperometry. Although b2LOxS gained the increased K_m value, the impact was not enough to expand the linear range in the DET-type enzyme electrode format, as this showed almost identical lactate concentration dependent current increase as the one with b2LOx, revealing the rate limiting step of this electrode is electron transfer from heme to electrode (Supplemental Materials Fig. S5). In order to expand the linear range of DET-type enzyme electrode, an outer membrane was applied to the electrode to make diffusion limit for reductive half-reaction of enzymatic reaction to improve the linear range.

The results are shown in Fig. 4A and B. After coating with an outer membrane, enzyme electrodes with b2LOx showed current increase up to 10 mM lactate (Fig. 4A red line and B red dots), which was a significant improvement compared with the one without an outer membrane (Fig. 2). The linear range of b2LOx immobilized electrode with an outer membrane was calculated as 0.5–5 mM lactate with $R^2 = 0.9837$. However, due to the inherent substrate inhibition property of this enzyme, the current decreased at lactate concentration higher than 10 mM. The enzyme electrode with b2LOxS, which obtained increased K_m value and waived from substrate inhibition, also showed drastic increase of lactate concentration range where current increase observed up to 50 mM. Most remarkably, unlike the electrode with b2LOx, this electrode did not show decrease in response at lactate concentration higher than 20 mM, which was due to the relief from substrate inhibition caused by the mutation of A95S. From the calibration curves (Fig. 4B), the b2LOxS immobilized electrode showed the linear range between 0.5 and 10 mM lactate with $R^2 = 0.9973$, the sensitivity of 21 nA/mM·mm^2, and a limit of detection (LOD) of 0.32 mM (3.3 × standard deviation/slope). At the 0.1 and 0.2 mM lactate, current changes were not confirmed compared with the background currents before addition of lactate. These results indicated DET-type lactate enzyme sensor was developed with expanded dynamic range by employing b2LOxS together with an outer membrane.

Table 1
Kinetic parameters of engineered enzymes.

Dehydrogenase activity				
	K_m (mM)	V_{max} (U/mg)	V_{max}/K_m (U/mg·mM)	K_i(mM)
AvLOx A96L/N212K[a]	1.1	170	160	330
AvLOx A95S/A96L/N212K	7.9	99	12	N.D.
b2LOx[a,b]	0.56	74	130	690
b2LOxS[c]	8.6	100	12	N.D.

N.D.: not detected.

[a] K_m and V_{max} values were calculated by the dehydrogenase activities for less than 20 mM lactate concentration and K_i values were calculated by the dehydrogenase activities for 20 mM or more lactate.

[b] b2LOx is a fusion enzyme AvLOx A96L/N212K mutant and Fcb2 heme domain.

[c] b2LOxS is a fusion enzyme AvLOx A95S/A96L/N212K mutant and Fcb2 heme domain.

3.4. Simultaneous lactate and glucose monitoring in the artificial sweat using flexible thin-film electrode and DET-type enzymes

Simultaneous lactate and glucose monitoring was attempted in the artificial sweat with the flexible thin-film electrodes (Fig. 5A) using b2LOxS and DET-type FADGDH, BcGDH. Fig. 5B shows the amperogram and Fig. 5C and D show the calibration curves calculated from Fig. 5B. The amperogram has been filtered to reduce the noise generated by the magnetic stirrer. The calibration curves were plotted using the peak current at each substrate concentration. The addition of lactate sample in the artificial sweat resulted in current increase in the lactate sensor with lactate concentration up to 50 mM, and the current increase was observed only from WE4 where b2LOxS was immobilized. The linear range for lactate detection was 0.5–20 mM ($R^2 = 0.963$) with LOD of 0.41 mM. The calculated sensitivities for lactate were 4.1 nA/mM·mm^2. The addition of glucose in the reaction solution also resulted current increase in the glucose sensor with glucose concentration up to 10 mM, and the current increase was observed only from WE3 where BcGDH was immobilized. The linear range for glucose detection was 0.1–5 mM ($R^2 = 0.950$) with LOD of 0.057 mM. The calculated sensitivities for glucose were 56 nA/mM·mm^2. These results demonstrated that a multiplexed DET-type enzyme sensor for lactate and glucose simultaneous measurements was constructed by developing an engineered LOx capable of DET by fusing Fcb2 heme domain and introducing mutation to relief substrate inhibition with increased K_m value, and by the combination of an outer membrane with DET-type glucose dehydrogenase.

Fig. 6 (A) shows the impact of electrochemically active ingredients, ascorbic acid, acetaminophen (paracetamol) and uric acid on sensor response toward 5 mM lactate and 1 mM glucose. The addition of these electrochemically active ingredients to the artificial sweat solution, did not significantly affect the sensor response. The bias values caused by these electrochemically active ingredients are almost within the SD values for sensor response toward 5 mM lactate and 1 mM glucose (Supplemental Materials, Table S3). Therefore, these results suggested that the presence of these electrochemically active ingredients was negligible in the sensor response. Fig. 6 (B) shows the results of the continuous operation of DET-type enzyme sensor investigated in the artificial sweat. Continuous operation of sensors revealed that the lactate sensor with newly developed engineered DET-type lactate oxidase, b2LOxS, showed the sensor signal decreased to 50% after 6.5 h continuous operation, whereas the glucose sensor with DET-type GDH was stable for the period we investigated (12 h).

4. Discussion

In this paper, we reported the creation of DET-type lactate sensing enzyme with expanded dynamic range, and to realize multiplexed DET-type lactate and glucose sensors with the combination of DET-type FADGDH. Considering increasing interest in the development of wearable lactate sensor, the development of DET-type lactate sensing enzyme will offer an ideal platform technology which is waived from complicated electrode structure, negligible impact of oxygen and electrochemical ingredients. However, the limitation of availability DET-type enzyme catalyzing oxidation of L-lactate was the key issue. An yeast derived L-lactate dehydrogenase, flavocytochrome b_2 (Fcb2), was reported to show DET with electrode (Smutok et al., 2017). However, Fcb2 was reported that this enzyme is inherently very fragile unstable in a wet condition (Bach et al., 1946), although its heme domain is stable

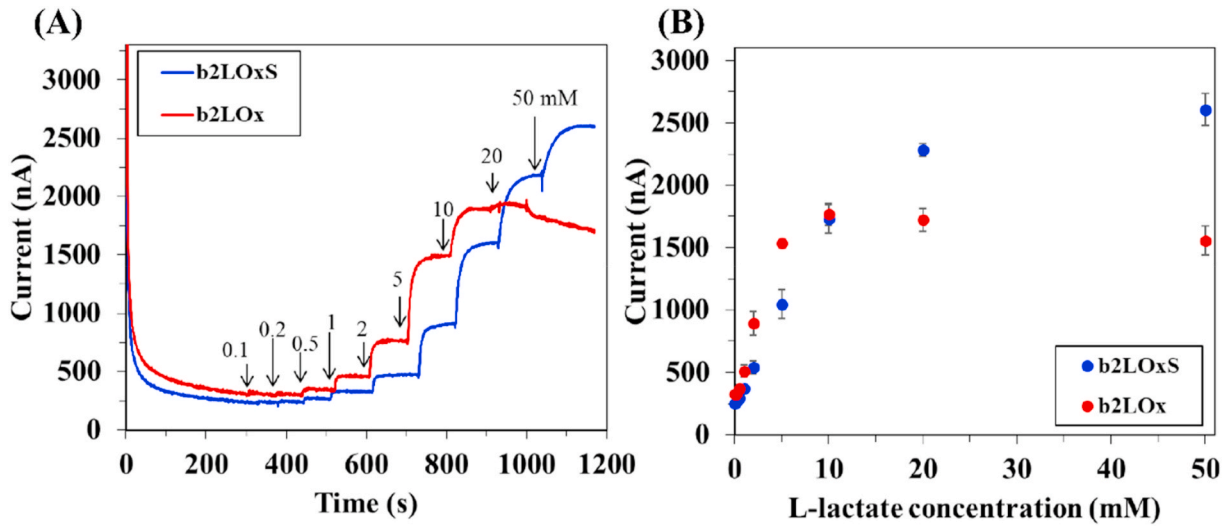

Fig. 4. L-lactate measurement based on chronoamperometry with an outer membrane. Chronoamperometry was conducted using the 10 mL of 20 mM P.P.B. pH 7.0 at 37 °C with continuous stirring. Applied potential was 150 mV vs. Ag/AgCl. Chronoamperograms using b2LOx (red) b2LOxS (blue) immobilized electrode with an outer membrane were shown in (A) and calibration curves were calculated as (B). These experiments were performed by using three different electrodes and error bars showed standard deviation.

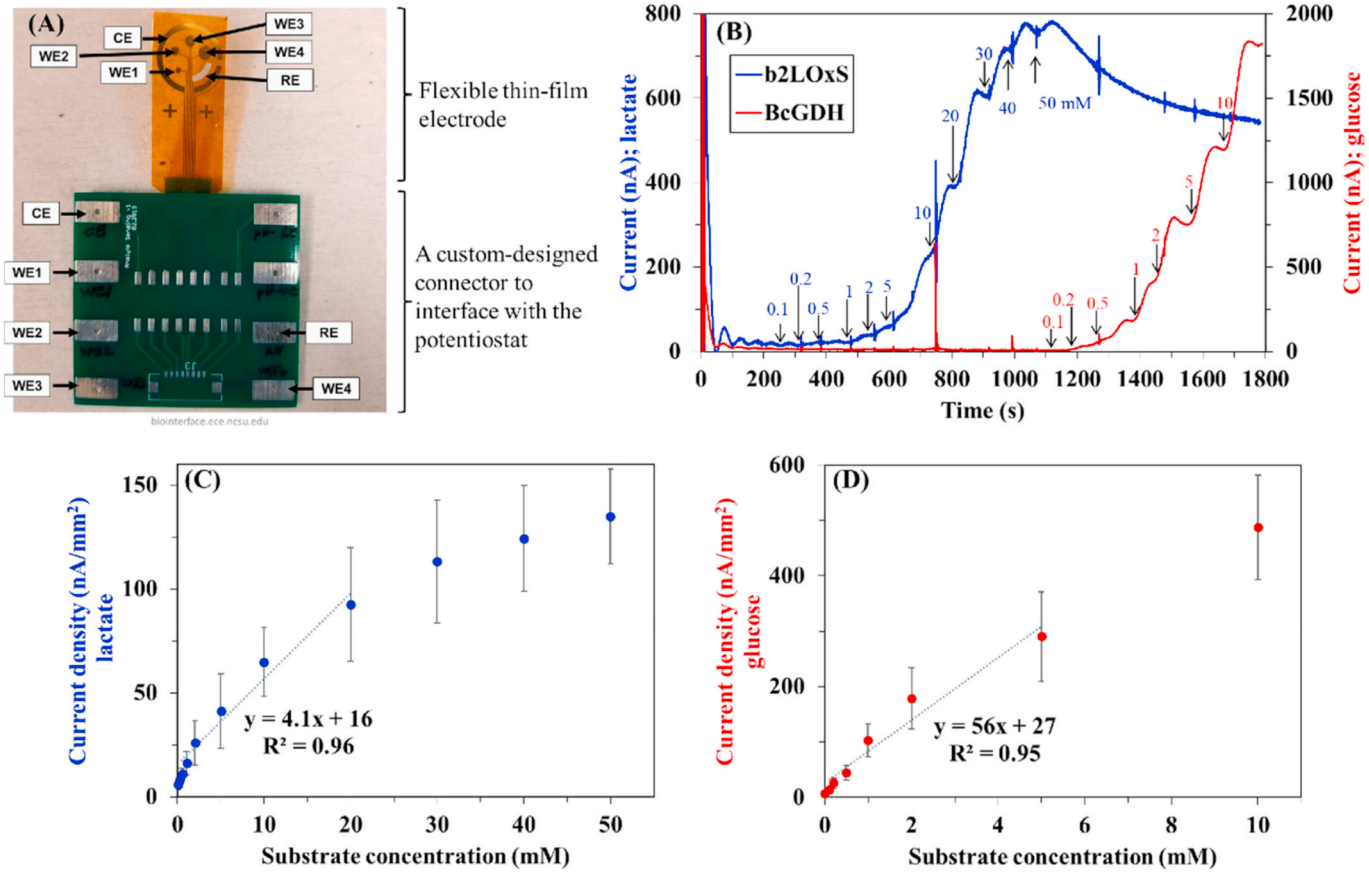

Fig. 5. Dual sensing for lactate and glucose with flexible thin-film electrode in the artificial sweat. Chronoamperometry was conducted with the fabricated thin-film electrode in 10 mL of artificial sweat pH 5.4 at 37 °C (150 mV vs. Ag/AgCl under continuous stirring). (A) Image of the flexible thin film electrode. This electrode was composed of 4 gold working electrodes, Ag/AgCl ink reference electrode and gold counter electrode. The b2LOxS was immobilized on WE4 (radius: 1.225 mm) and BcGDH was immobilized on WE3 (radius: 0.975 mm). Chronoamperogram was shown in (B) and calibration curves were calculated as (C) for lactate and (D) for glucose. Blue line and marker showed the result of b2LOxS immobilized electrode and red line and marker showed the result of BcGDH immobilized electrode. Chronoamperogram was performed smoothing process by EC-Lab software (Bio-Logic Science Instruments Ltd., Seyssinet-Pariset, France). Error bars showed standard deviations in the results of different three electrodes.

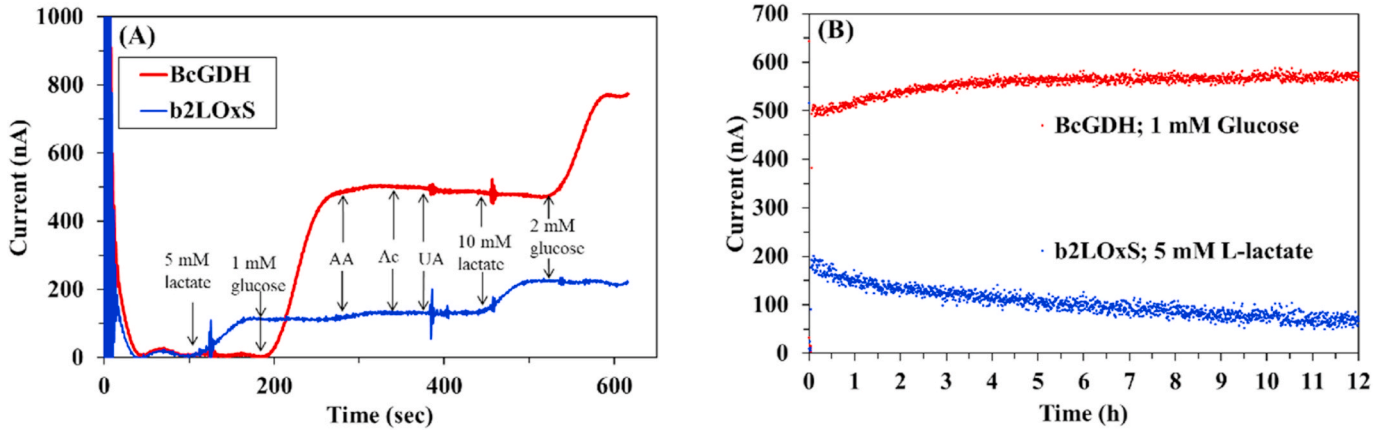

Fig. 6. Investigation of electrochemical interferents impact on sensor responses and sensor continuous operation in artificial sweat. (A) Amperometric responses against sweat interferents in artificial sweat pH 5.4 at 37 °C and applied 150 mV vs. Ag/AgCl of applied potential under continuous stirring. The impact of 10 μM ascorbic acid, 132 μM acetaminophen, and 59 μM uric acid were investigated in the presence of 5 mM lactate or 1 mM glucose. The arrows indicated the points where each substrate was spiked in the artificial sweat. Chronoamperogram was performed smoothing process by EC-Lab software (Bio-Logic Science Instruments Ltd., Seyssinet-Pariset, France). (B) Continuous operation of the lactate and glucose dual sensing system in the artificial sweat pH 5.4 at 37 °C with applied oxidation potential of 150 mV vs. Ag/AgCl under continuous stirring with 5 mM lactate and 1 mM glucose. Blue line and marker showed the result of b2LOxS immobilized electrode and red line and marker showed the result of BcGDH immobilized electrode.

(Labeyrie et al., 1978). In addition, K_m value of Fcb2 was reported as 0.5 mM (Black et al., 1989) which is not suitable for the monitoring of lactate in sweat. Considering that current commercially available enzyme sensors for L-lactate employ LOx, due to its stability and substrate specificity (Hiraka et al., 2018), we planned to develop DET-type lactate sensing enzyme based on LOx. Therefore, DET-type lactate sensing enzyme was created by constructing a fusion enzyme, b2LOx, which is composed of AvLOx A96L/N212K mutant and Fcb2 heme domain. This fusion enzyme showed intra-electron transfer between FMN to heme (Fig. 1), and showed DET ability with gold electrode (Fig. 2). Recently, we reported the fusion enzymes composed of non-DET-type fungi derived FADGDH with heme *b* containing proteins, heme *b* domain of cellobiose dehydrogenase (Ito et al., 2019a) and cytochrome b_{562} (Yanase et al., 2020). FADGDH belongs to the group called glucose-methanol-choline oxidoreductase, monomeric enzyme, and they are the enzymes with totally different structures compared with FMN harboring oxidoreductase group including LOx, which is homo-tetrameric enzyme. This study was the first report demonstrating that non-DET-type FMN enzyme can be also converted into DET-type enzyme by fusing heme protein, in spite of significant difference in the structure between FADGDH and LOx. Moreover, the addition of DET ability in LOx was only available for LOx mutants which was minimized their ability to utilize oxygen as the primary electron acceptor.

However, according to the result of chronoamperometry with b2LOx immobilized electrode (Fig. 2), the response current against lactate did not increase at lactate concentration higher than 1 mM, because the electron transfer from b2LOx to electrode was considered as a rate-limiting step. This would be due to the low K_m value of LOx, substrate inhibition and rate limiting step of the reaction is supposed to be electron transfer from enzyme to electrode.

To overcome the limited linear range of b2LOx immobilized electrodes, we first attempted the mutagenesis of this enzyme to increase K_m value and to relieve the substrate inhibition. Ala95 of AvLOx was focused according to the previous report suggesting the role in AvLOx reaction mechanism (Yorita et al. (1996). They reported that AvLOx A95G mutant resulted 10 times increase in the dissociation constant for L-lactate, indicating Ala95 is a crucial residue for not only substrate recognition but also substrate releasing. Considering the reported A95G mutation showed extended substrate specificity, therefore, alternate A95 substitutions were investigated. Among investigated Ala95 substitutions into little bulky amino acid residues (Cys, Ser, Val, Thr, Pro) in AvLOx A96L/N212K mutant, only AvLOx A95S/A96L/N212K mutant kept dye-mediated lactate dehydrogenase activity after the mutation, and showed the increased K_m values with relieved substrate inhibition without loss of the substrate specificity. A95S substitution might provide the steric hindrance in active site but might not affect the other amino acid residue for lactate recognition such as Tyr40, Tyr146, Tyr215, His265 and Arg268. Consequently, A95S mutation may allow to release substrate easily and relieve the substrate inhibition with extending the K_m value (Table 1). Then, we integrated AvLOx A95S mutation and b2LOx. The newly constructed b2LOxS immobilized electrode expand the linear range up to 10 mM, thanks to its extended K_m value (8.6 mM) compared with the one of b2LOx (0.56 mM).

Since A95S mutation alone did not realize the extended linear range when the enzyme electrode was investigated with this mutant, we attempted to use an outer membrane to limit the substrate diffusion. Compared with the results of chronoamperometry of b2LOx immobilized electrode with or without an outer membrane (Figs. 2 and 4), the outer membrane increased the linear range upper limit from 0.5 mM (R^2 = 0.9773) to 5 mM (R^2 = 0.9837). The outer membrane successfully worked to limit the substrate diffusion and expand the linear range 10-fold. The combination of the employment of an outer membrane together with A95S mutation realized the further expand of linear range of lactate sensing, up to 10 mM (R^2 = 0.9973), mainly due to the elimination of LOx inherent substrate inhibition property by A95S mutation.

Finally, multiplexed lactate and glucose DET-type amperometric sensor was constructed with the combination of flexible film electrode covered by an outer membrane. The sensor performances, such as the responses toward lactate and glucose, the impact of electrochemical interferants, and continuous operation were evaluated in the artificial sweat. The results revealed that the constructed sensors showed relevant signals toward physiological concentration range of lactate and glucose, even in the artificial sweat. The sensor signals from both the one with b2LOx and DET-type GDH, were lower than the ones observed in a potassium phosphate buffer (pH 7.0) solution (Supplemental Materials, Fig. S6). The decrease in the sensor responses would be mainly attributed to the pH of artificial sweat (pH 5.4), considering optimum pH for enzymes are around neutral pH. The impact of the presence of electrochemical interferants (ascorbic acid, acetaminophen and uric acid) which may exist in sweat sample, was revealed to be negligible. In this study, the sensors were operated at +150 mV vs Ag/AgCl. This is the one of the benefits of DET-type enzyme based sensing, which allows the relatively low oxidation potential for the operation. Continuous

operation of sensors revealed that the lactate sensor with newly developed engineered DET-type lactate oxidase, b2LOxS, showed the sensor signal decreased to 50% after 6.5 h continuous operation, whereas the glucose sensor with DET-type GDH was stable for the period we investigated (12 h). Considering that the result of continuous operation of the lactate sensor with b2LOxS in a buffer solution at pH 7.0 kept its initial response at least over 6 h of continuous operation (Supplementary Materials, Fig. S7), the decrease in the signal of lactate sensor in the artificial sweat would be due to the low pH of artificial sweat which would inactivate b2LOxS. We believe that further engineering of b2LOxS to increase the stability will improve the operational stability of lactate sensor.

To the best of our knowledge, this is the first report of an enzymatic sensor to achieved the simultaneous measurement of lactate and glucose based on the DET principle. Thanks to the DET-type enzymes, no cross-talking error was observed. Moreover, our constructed lactate sensor showed the comparable sensing property to the other LOx-based flexible thin-film amperometric lactate sensors owing to the mutation (Table 2). Although further expansion of the linear range for lactate measurement is required to cover the sweat lactate concentration (Harvey et al., 2010), the optimization of the outer membrane thickness will solve this issue. Moreover, the integration of this DET-type dual sensing system and recently reported sweat sampler system (Yokus et al., 2019) will enable the realization of wearable multiplexed biosensors for longitudinal, simultaneous monitoring of sweat lactate and glucose.

5. Conclusion

A new lactate sensing element, b2LOxS was designed for development of DET-type multiplexed biosensing system. To obtain the DET ability, the oxygen insensitive AvLOx mutant was fused with Fcb2 heme domain. The designed fusion enzyme b2LOx was immobilized onto Au-disk electrodes and showed an amperometric response to lactate without any external electron mediator. However, the linear range was limited by rather low electron transfer efficiency from enzyme to electrode and substrate inhibition with low K_m value of b2LOx. Therefore, we attempted to relieve the substrate inhibition by site-directed mutagenesis together with the employment of an outer membrane to limit the substrate diffusion and consequently increase the linear range. AvLOx A95S/A96L/N212K mutant was newly designed and fused with Fcb2 heme domain. This novel fusion enzyme b2LOxS relieved the substrate inhibition until 100 mM L-lactate and expanded the K_m value from 0.56 mM to 8.6 mM without loss of the substrate specificity. Moreover, b2LOxS immobilized electrodes coated with a cellulose acetate outer membrane expanded the linear range up to 10 mM without substrate inhibition. Finally, b2LOxS and BcGDH were immobilized onto the flexible thin-film electrodes, and evaluated their performance in the artificial sweat. The sensors achieved simultaneous detection of lactate and glucose without cross-talking error, with the detected linear ranges of 0.5–20 mM for lactate and 0.1–5 mM for glucose, sensitivities of 4.1 nA/mM·mm^2 for lactate and 56 nA/mM·mm^2 for glucose, and limit of detections of 0.41 mM for lactate and 0.057 mM for glucose. The impact of the presence of electrochemical interferants (ascorbic acid, acetaminophen and uric acid), was revealed to be negligible. Continuous operation of sensors revealed that the lactate sensor with newly developed engineered DET-type lactate oxidase, showed the sensor signal decreased to 50% after 6.5 h continuous operation, whereas the glucose sensor with DET-type GDH was stable for the period we investigated (12 h). Considering that the result of continuous operation of the lactate sensor with b2LOxS in a buffer solution at pH 7.0 kept its initial response at least over 6 h of continuous operation, further engineering to improve at lower pH will enhance the operational stability of lactate sensor. This is the first report of lactate and glucose dual sensing system based on the DET principle and this system showed the comparable property to other reported LOx-based flexible thin-film amperometric lactate sensors. Considering the sweat lactate or glucose concentration range, further improvement of linear range for lactate and glucose is required by the optimization of the fabrication method, but the integration of this DET-type sensing system and sophisticated sweat sampler system will realize the wearable multiplexed biosensor for sweat.

Author contributions

Hiraka, Tsugawa, Asano, Yokus, Ikebukuro, Daniele, Sode: Study conception and design. Hiraka: Data acquisition. Yokus, Daniele: Flexible thin-film electrode fabrication. Hiraka, Tsugawa, Yokus, Daniele, Sode: Analysis and interpretation of data. Hiraka, Yokus, Daniele, Sode: Drafting of manuscript.

Table 2
Comparison of LOx-based flexible thin-film amperometric lactate sensors.

Electrode/Modification	Principle	Sensitivity (μA/mM·cm^2)	Linear range (mM)	LOD (mM)	Applied potential (V vs. Ag/AgCl)	Reference
Au/PB/Chitosan-CNT/LOx/Chitosan-CNT	1st gen.	3.1	~30	NR	0	Gao et al. (2016)
PB/LOx-BSA-Chitosan/PVC	1st gen.	1.28	~28	NR	−0.1	Imani et al. (2016)
AgNP/Nafion/LOx-BSA-GA	1st gen.	0.256	1–25	NR	0.65	Abrar et al. (2016)
CNT/LOx-GA	1st gen.	0.358 (μA/mM)	0.0476–1.52	0.0025	0.6	Luo et al. (2018)
Au/PB/Chitosan-CNT/LOX/Chitosan-CNT	1st gen.	0.395 (μA/mM)	0.05–0.85	NR	0.6	Ashley et al. (2019)
CNT-$Ti_3C_2T_x$-PB/Chitosan-LOx-BSA-GA	1st gen.	11.4	~22	0.00067	−0.1	Lei et al. (2019)
SilkNCT-PtNP/LOx/Chitosan	1st gen.	2.46	5–35	0.5	−0.2	He et al. (2019)
Au/AuNP/PB/LOx-BSA/GA/Nafion	1st gen.	1.49	5–20	NR	−0.1	Yokus et al. (2020)
PB/Chitosan/LOx-Chitosan	1st gen.	0.9 (μA/mM)	~12.5	NR	−0.06	Terse-Thakoor et al. (2020)
Au/PB/LOx/Chitosan	1st gen.	19.13	~5	0.137	−0.1	Wang et al. (2021)
Carbon ink/TTF-CNT/LOx/Chitosan/GA	2nd gen.	10.31	1–20	NR	0.05	Jia et al. (2013)
Buckypaper/$FcMe_2$-LPEI-LOx-EGDGE	2nd gen.	400	~5	0.001	0.3 (vs. SCE)	Hickey et al. (2016)
Au/TTF-CNT/LOx-Chitosan-CNT	2nd gen.	68	~24	NR	NR	Payne et al. (2019)
Au/CNT/b2LOxS/PEI-PEGDGE/CA	**3rd gen.**	**0.41**	**0.5–20**	**0.41**	**0.15**	**This work**

NR: not reported.
PB: Prussian blue, CNT: carbon nanotube, BSA: bovine serum albumin, SilkNCT: silk fabric-derived intrinsically nitrogen-doped carbon textile, PtNP: platinum nanoparticle, AuNP: Au nanoparticle, GA: glutaraldehyde, TTF: tetrathiafulvalene, $FcMe_2$-LPEI: dimethylferrocene-modified linear poly(ethylenimine), EGDGE: ethylene glycol diglycidyl ether, PEI: poly(ethylenimine), PEGDGE:polyethylene glycol diglycidyl ether, CA: cellulose acetate.

Declaration of competing interest

The authors declare that they have no known competing financial interests or personal relationships that could have appeared to influence the work reported in this paper.

Acknowledgements

This work was done in collaboration with the National Science Foundation (EEC1160483) through a NSF Nanosystems Engineering Research Center (NERC) for Advanced Self-Powered Systems of Integrated Sensors and Technologies (ASSIST). K. H. was financially supported by the Nakatani Foundation for Advancement of Measuring Technologies in Biomedical Engineering.

Appendix A. Supplementary data

Supplementary data to this article can be found online at https://doi.org/10.1016/j.bios.2020.112933.

References

Abrar, M.A., Dong, Y., Lee, P.K., Kim, W.S., 2016. Sci. Rep. 6 (1), 30565.
Anastasova, S., Crewther, B., Bembnowicz, P., Curto, V., Ip, H.M.D., Rosa, B., Yang, G.-Z., 2017. Biosens. Bioelectron. 93, 139–145.
Ashley, B.K., Brown, M.S., Park, Y., Kuan, S., Koh, A., 2019. Biosens. Bioelectron. 132, 343–351.
Bach, S.J., Dixon, M., Zerfas, L.G., 1946. Biochem. J. 40 (2), 229–239.
Bakker, J., Nijsten, M.W.N., Jansen, T.C., 2013. Ann. Intensive Care 3, 12-12.
Black, M.T., White, S.A., Reid, G.A., Chapman, S.K., 1989. Biochem. J. 258 (1), 255–259.
Brunt, C.E., Cox, M.C., Thurgood, A.G.P., Moore, G.R., Reid, G.A., Chapman, S.K., 1992. Biochem. J. 283 (1), 87–90.
Clark Jr., L.C., Noyes, L.K., Grooms, T.A., Moore, M.S., 1984. Crit. Care Med. 12 (5), 461–464.
Currano, L.J., Sage, F.C., Hagedon, M., Hamilton, L., Patrone, J., Gerasopoulos, K., 2018. Sci. Rep. 8 (1), 15890.
Faude, O., Kindermann, W., Meyer, T., 2009. Sports Med. 39 (6), 469–490.
Ferri, S., Kojima, K., Sode, K., 2011. J. Diabetes Sci. Technol. 5 (5), 1068–1076.
Gao, W., Emaminejad, S., Nyein, H.Y.Y., Challa, S., Chen, K., Peck, A., Fahad, H.M., Ota, H., Shiraki, H., Kiriya, D., Lien, D.-H., Brooks, G.A., Davis, R.W., Javey, A., 2016. Nature 529 (7587), 509–514.
Harvey, C.J., LeBouf, R.F., Stefaniak, A.B., 2010. Toxicol. Vitro 24 (6), 1790–1796.
He, W., Wang, C., Wang, H., Jian, M., Lu, W., Liang, X., Zhang, X., Yang, F., Zhang, Y., 2019. Sci. Adv. 5 (11), eaax0649.
Hickey, D.P., Reid, R.C., Milton, R.D., Minteer, S.D., 2016. Biosens. Bioelectron. 77, 26–31.
Hiraka, K., Kojima, K., Lin, C.-E., Tsugawa, W., Asano, R., La Belle, J.T., Sode, K., 2018. Biosens. Bioelectron. 103, 163–170.
Hiraka, K., Kojima, K., Tsugawa, W., Asano, R., Ikebukuro, K., Sode, K., 2020a. Biosens. Bioelectron. 151, 111974.
Hiraka, K., Tsugawa, W., Sode, K., 2020b. Int. J. Mol. Sci. 21 (11), 3797.
Horaguchi, Y., Saito, S., Kojima, K., Tsugawa, W., Ferri, S., Sode, K., 2012. Int. J. Mol. Sci. 13 (11), 14149–14157.
Horaguchi, Y., Saito, S., Kojima, K., Tsugawa, W., Ferri, S., Sode, K., 2014. Electrochim. Acta 126, 158–161.
Imani, S., Bandodkar, A.J., Mohan, A.M.V., Kumar, R., Yu, S., Wang, J., Mercier, P.P., 2016. Nat. Commun. 7 (1), 11650.
Inose, K., Fujikawa, M., Yamazaki, T., Kojima, K., Sode, K., 2003. Biochim. Biophys. Acta Protein Proteonomics 1645 (2), 133–138.
Ito, K., Okuda-Shimazaki, J., Mori, K., Kojima, K., Tsugawa, W., Ikebukuro, K., Lin, C.-E., La Belle, J., Yoshida, H., Sode, K., 2019a. Biosens. Bioelectron. 123, 114–123.
Ito, Y., Okuda-Shimazaki, J., Tsugawa, W., Loew, N., Shitanda, I., Lin, C.-E., La Belle, J., Sode, K., 2019b. Biosens. Bioelectron. 129, 189–197.
Jia, W., Bandodkar, A.J., Valdés-Ramírez, G., Windmiller, J.R., Yang, Z., Ramírez, J., Chan, G., Wang, J., 2013. Anal. Chem. 85 (14), 6553–6560.
Karpova, E.V., Laptev, A.I., Andreev, E.A., Karyakina, E.E., Karyakin, A.A., 2020. ChemElectroChem 7 (1), 191–194.
Karube, I., Matsunaga, T., Teraoka, N., Suzuki, S., 1980. Anal. Chim. Acta 119 (2), 271–276.
Kenausis, G., Taylor, C., Katakis, I., Heller, A., 1996. J. Chem. Soc., Faraday Trans. 92 (20), 4131–4136.
Kim, S., Nibe, E., Ferri, S., Tsugawa, W., Sode, K., 2010. Biotechnol. Lett. 32 (8), 1123–1129.
Kim, S., Nibe, E., Tsugawa, W., Kojima, K., Ferri, S., Sode, K., 2012. Biotechnol. Lett. 34 (3), 491–497.
Kojima, K., Kobayashi, T., Tsugawa, W., Ferri, S., Sode, K., 2013. J. Mol. Catal. B Enzym. 88, 41–46.
Kondoh, Y., Kawase, M., Ohmori, S., 1992. Eur. J. Appl. Physiol. Occup. Physiol. 65 (1), 88–93.
Labeyrie, F., Baudras, A., Lederer, F., 1978. [27] Flavocytochrome b2 or l-lactate cytochrome c reductase from yeast. In: Fleischer, S., Packer, L. (Eds.), Methods Enzymol. Academic Press, pp. 238–256.
Lee, H., Song, C., Hong, Y.S., Kim, M.S., Cho, H.R., Kang, T., Shin, K., Choi, S.H., Hyeon, T., Kim, D.-H., 2017. Sci. Adv. 3 (3), e1601314.
Lee, I., Loew, N., Tsugawa, W., Ikebukuro, K., Sode, K., 2019. Biosens. Bioelectron. 124–125, 216–223.
Lee, I., Loew, N., Tsugawa, W., Lin, C.-E., Probst, D., La Belle, J.T., Sode, K., 2018. Bioelectrochemistry 121, 1–6.
Lei, Y., Zhao, W., Zhang, Y., Jiang, Q., He, J.-H., Baeumner, A.J., Wolfbeis, O.S., Wang, Z. L., Salama, K.N., Alshareef, H.N., 2019. Small 15 (19), 1901190.
Lin, C.-E., Hiraka, K., Matloff, D., Johns, J., Deng, A., Sode, K., La Belle, J., 2018. Sensor. Actuator. B Chem. 270, 525–529.
Liu, G., Alomari, M., Sahin, B., Snelgrove, S.E., Edwards, J., Mellinger, A., Kaya, T., 2015. Appl. Phys. Lett. 106 (13), 133702.
Luo, X., Shi, W., Yu, H., Xie, Z., Li, K., Cui, Y., 2018. Sensors 18 (10), 3398.
Maeda-Yorita, K., Aki, K., Sagai, H., Misaki, H., Massey, V., 1995. Biochimie 77 (7–8), 631–642.
Matsunaga, T., Karube, I., Teraoka, N., Suzuki, S., 1982. Appl. Microbiol. Biotechnol. 16 (2), 157–160.
Mitsubayashi, K., Suzuki, M., Tamiya, E., Karube, I., 1994. Anal. Chim. Acta 289 (1), 27–34.
Mizock, B.A., Falk, J.L., 1992. Crit. Care Med. 20 (1), 80–93.
Palleschi, G., Turner, A.P.F., 1990. Anal. Chim. Acta 234, 459–463.
Payne, M.E., Zamarayeva, A., Pister, V.I., Yamamoto, N.A.D., Arias, A.C., 2019. Sci. Rep. 9 (1), 13720.
Sempionatto, J.R., Nakagawa, T., Pavinatto, A., Mensah, S.T., Imani, S., Mercier, P., Wang, J., 2017. Lab Chip 17 (10), 1834–1842.
Smutok, O., Karkovska, M., Serkiz, R., Vus, B., Čenas, N., Gonchar, M., 2017. Sensor. Actuator. B Chem. 250, 469–475.
Sode, K., Tsugawa, W., Yamazaki, T., Watanabe, M., Ogasawara, N., Tanaka, M., 1996. Enzym. Microb. Technol. 19 (2), 82–85.
Taurino, I., Reiss, R., Richter, M., Fairhead, M., Thöny-Meyer, L., De Micheli, G., Carrara, S., 2013. Electrochim. Acta 93, 72–79.
Terse-Thakoor, T., Punjiya, M., Matharu, Z., Lyu, B., Ahmad, M., Giles, G.E., Owyeung, R., Alaimo, F., Shojaei Baghini, M., Brunyé, T.T., Sonkusale, S., 2020. npj Flex. Electron. 4 (1), 18.
Treu, B.L., Minteer, S.D., 2008. Bioelectrochemistry 74 (1), 73–77.
Tsuya, T., Ferri, S., Fujikawa, M., Yamaoka, H., Sode, K., 2006. J. Biotechnol. 123 (2), 127–136.
Wang, R., Zhai, Q., An, T., Gong, S., Cheng, W., 2021. Talanta 222, 121484.
Yamashita, Y., Ferri, S., Huynh, M.L., Shimizu, H., Yamaoka, H., Sode, K., 2013. Enzym. Microb. Technol. 52 (2), 123–128.
Yamashita, Y., Lee, I., Loew, N., Sode, K., 2018. Curr. Opin. Electrochem. 12, 92–100.
Yamazaki, T., Okuda-Shimazaki, J., Sakata, C., Tsuya, T., Sode, K., 2008. Anal. Lett. 41 (13), 2363–2373.
Yanase, T., Okuda-Shimazaki, J., Mori, K., Kojima, K., Tsugawa, W., Sode, K., 2020. Biochem. Biophys. Res. Commun. 530 (1), 82–86.
Yokus, M.A., Saha, T., Fang, J., Dickey, M.D., Velev, O.D., Daniele, M.A., 2019. 2019 IEEE SENSORS 27-30 Oct. 2019. IEEE, INSPEC Accession Number, pp. 1–4, 19278490.
Yokus, M.A., Songkakul, T., Pozdin, V.A., Bozkurt, A., Daniele, M.A., 2020. Biosens. Bioelectron. 153, 112038.
Yorita, K., Aki, K., Ohkuma-Soyejima, T., Kokubo, T., Misaki, H., Massey, V., 1996. J. Biol. Chem. 271 (45), 28300–28305.
Yoshida, H., Kojima, K., Shiota, M., Yoshimatsu, K., Yamazaki, T., Ferri, S., Tsugawa, W., Kamitori, S., Sode, K., 2019. Acta Crystallogr. D Struct. Biol. 75 (9), 841–851.